

# Advancing Lunar Exploration: The Neutral Gas Mass Spectrometer for Regolith and Exosphere Analysis

Rico Fausch  
Physics Institute, University of Bern,  
Sidlerstrasse 5, 3012 Bern  
Switzerland  
rico.fausch@unibe.ch

Lukas Hofer  
Physics Institute, University of Bern,  
Sidlerstrasse 5, 3012 Bern  
Switzerland  
lukas.hofer@gmail.com

Davide Lasi  
Physics Institute, University of Bern,  
Sidlerstrasse 5, 3012 Bern  
Switzerland  
davide.lasi@gmail.com

Peter Wurz  
Physics Institute, University of Bern,  
Sidlerstrasse 5, 3012 Bern  
Switzerland  
peter.wurz@unibe.ch

Hans Rudolf Elsener  
Empa, Swiss Federal Laboratories  
for Materials Science and  
Technology, Dübendorf, Switzerland  
HansRudolf.Elsener@empa.ch

Jürg Jost  
Physics Institute, University of Bern,  
Sidlerstrasse 5, 3012 Bern  
Switzerland  
juerg.jost@spacetek.ch

Daniele Piazza  
Physics Institute, University of Bern,  
Sidlerstrasse 5, 3012 Bern  
Switzerland  
daniele.piazza@unibe.ch

**Abstract**—The Neutral Gas Mass Spectrometer (NGMS) for the Luna 25 and Luna 27 missions represents a pivotal advancement in lunar exploration technology. This compact time-of-flight (TOF) spaceborne instrument is integrated with a gas chromatograph (GC) and a pyrolysis oven, designed to investigate the chemical composition of volatiles in the lunar polar regolith and the tenuous lunar exosphere. NGMS measures element, isotope, and molecular compositions, including CHON compounds, water, and noble gases. It features a robust design with an ion storage source, redundant thermionic electron emitters, pulsed ion extraction, ion drift paths, an ion mirror, and a high-speed microchannel plate detector, achieving a mass resolution better than 1000 and a dynamic range of up to 6 decades within a 1-second integration time. Preparations for the mission included the successful coupling of the TOF-MS with GC, enabling chemical pre-separation of species. Test measurements with hydrocarbons and noble gases confirmed the system's high sensitivity and extensive dynamic range, with detection limits for volatile species in lunar regolith estimated at  $2 \cdot 10^{-10}$  by mass for hydrocarbons and  $2 \cdot 10^{-9}$  by mass for noble gases. The NGMS design ensures high sensitivity with moderate resource requirements, recording all masses simultaneously. The instrument's control electronics were developed to meet stringent mission requirements, including a maximum power consumption of 23 W, compact size, and radiation tolerance, all assessed at technical readiness level 8. The complete instrument weighs 3.2 kg. This outstanding compact design was achieved by creating a miniaturized, integrated ion optical system, relying on a metal-ceramic brazed structure rather than discrete ion optical elements. By omitting bulky connecting components, a narrow opening angle of the ion beam inside the ion optical system was possible, minimizing ion optical aberrations.

Although NGMS ultimately did not fly to the Moon due to programmatic considerations, its architectural baseline continues to shape ongoing advances in lunar and planetary exploration. Thanks to its exceptional achievements, it served as a baseline for the design of three instruments on board space missions: NIM on board ESA's JUICE mission and MANIaC on the Comet Interceptor mission, both specifically designed to analyze tenuous exospheres, and CODEX on board NASA's DIMPLE payload which is designed to analyze and date lunar rocks in situ.

## TABLE OF CONTENTS

1. INTRODUCTION AND SCIENCE OBJECTIVES.....	2
2. INSTRUMENT ARCHITECTURE .....	3
3. SCIENTIFIC PERFORMANCE .....	8
4. STATUS .....	9
5. IMPACT .....	10
6. SUMMARY .....	10
LIST OF ABBREVIATIONS, ACRONYMS, AND SYMBOLS .....	10
ACKNOWLEDGEMENTS .....	10
REFERENCES .....	11
BIOGRAPHY .....	13

## 1. INTRODUCTION AND SCIENCE OBJECTIVES

The exploration of the lunar south pole using in situ mass spectrometry has become a central focus in planetary science due to the potential presence of water ice and other volatiles within permanently shadowed regions. Moreover, the foreseen landing sites of the Artemis crewed missions are near the lunar south pole. Conducting measurements in this area is essential for quantifying the Moon's volatile inventory and assessing the distribution and origin of these compounds. Investigating these volatiles is crucial for understanding the Moon's geological history, including its formation, thermal evolution, and magmatic processes. Moreover, possible exogenic sources of volatiles (comets, meteorites, etc.) may contribute to the volatile inventory. The presence of water ice holds profound implications for future human exploration, potentially providing in situ resources for life support and fuel.

### *The joint ESA-Roscosmos Luna Program*

In the late nineties, the Russian space agency, Roscosmos devised a program for the scientific exploration of the Moon with a series of launches until 2020, as initial plans foresaw [1], [2]. Following the success of the Russian Luna program with its latest successful Luna 24 mission in 1976, the succeeding lander missions are referred to as Luna 25, also called Luna-Glob, and Luna 27, also called Luna-Resurs.

The plans foresaw that in early 2015, Luna 25 would have been launched as a Russian-built lander on board a Soyuz-2.1a rocket with a Fregat fourth stage. In 2017, the Luna 27 mission would have been sent to the Moon on board a Soyuz-2.1b rocket. The ambitious Luna program scenario foresaw four further launches of spacecraft to the Moon.

The two Luna 25 and 27 spacecraft would have been almost identical, with the difference of the possible addition of a small rover on board Luna 25, contributed by the Indian Space Research Organisation (ISRO). On board Luna 27, surface-drilling equipment was planned to be accommodated.

### *Luna 25*

The initial plans of the Luna 25 mission foresaw flying two mass spectrometers (MS) to the Moon, a Laser Ablation Mass Spectrometer (LASMA-LR) for elemental analysis of the regolith mineralogy [3] and a Neutral Gas Mass Spectrometer (NGMS) for the analysis of both the lunar regolith and exosphere. During the development phase of the hardware of the NGMS instrument, the Luna 25 mission was descopeped from a spearheading scientific mission carrying a rover to a technology demonstrating mission. Given the new goals of the mission, NGMS was also descopeped from this mission, despite most of the hardware being already available. Ultimately, the Luna 25 spacecraft was launched on board a Sojus-2.1b/Fregat-M with LASMA-LR on board on August 10, 2023. It performed a hard landing on the Moon some days later due to thruster malfunction.

### *Luna 27*

The Luna 27 mission is targeting the Moon's south polar regions [4], [5]. The mission aims to perform in-depth analysis of the lunar regolith and exosphere, focusing on the detection and characterization of lunar volatiles, the mineralogy of both the lunar surface regolith and excavated material to about 1 m depth [6], and assessment of in situ resource utilization (ISRU) potential [7].

Understanding the distribution and composition of lunar volatiles is crucial for reconstructing the Moon's geological history and assessing its resource potential (e.g., references [8], [9]). Early analyses of lunar samples from the Apollo and Luna missions indicated a virtually anhydrous Moon, with rocks exhibiting no evidence of water or hydrous minerals (e.g., reference [10] and references therein). This led to the long-held belief that the Moon was depleted in volatiles, influencing models of its formation and evolution.

However, advancements in remote sensing and analytical techniques have significantly altered this perspective. The Lunar Prospector mission detected enhanced fluxes of epithermal neutrons at the lunar poles, suggesting the presence of hydrogen-rich materials, potentially water ice, in permanently shadowed regions [11]. Subsequent missions, such as the Lunar Reconnaissance Orbiter (LRO) and the Lunar Crater Observation and Sensing Satellite (LCROSS), provided further evidence of water ice and other volatiles in these cold traps [12].

Spectroscopic observations from the Moon Mineralogy Mapper (M<sup>3</sup>) instrument on board Chandrayaan-1 revealed absorption features in infrared spectra near 2.8–3.0  $\mu\text{m}$  across the lunar polar surface, indicative of hydroxyl (OH) and possibly molecular water (H<sub>2</sub>O) [13], [14]. These findings suggest that solar wind protons interacting with oxygen-rich minerals could produce hydroxyl, and that water may be more widespread than previously thought.

Analyses of lunar volcanic glass beads from Apollo samples have revealed significant amounts of water within the lunar interior. Saal et al. [15] reported water contents up to 745 ppm in lunar volcanic glasses, suggesting that the lunar mantle may contain water at levels comparable to Earth's upper mantle. This discovery challenges the paradigm of a completely dry Moon and has significant implications for models of lunar origin and differentiation.

The potential presence of water ice and other volatiles at the lunar poles presents opportunities for in situ resource utilization, which involves harnessing and utilizing extraterrestrial resources to support space missions [9], [16]. Water ice can be processed to produce oxygen and hydrogen for life support systems and propellant, significantly reducing the reliance on Earth-supplied resources. ISRU is considered a critical component for sustainable lunar exploration and as a foundation for future crewed missions to Mars and beyond.

To achieve these scientific objectives, the Luna 27 mission is equipped with a Gas Analytic Package (GAP) [17], a suite of advanced instruments designed for in situ analysis of the lunar regolith and exosphere. GAP focuses on the detection and quantification of volatile compounds, including water, noble gases, and organic molecules. It consists of a sample handling and distribution system and analytical instruments including the Gas Chromatograph – Neutral Gas Mass Spectrometers (GC–NGMS).

#### *NGMS as Part of GAP – Lunar Regolith*

The main scientific goals that are planned to be achieved by the application of the gas chromatograph mass spectrometer complex are:

- Investigation of chemical composition and inventory of volatiles (water, CO<sub>2</sub>, N<sub>2</sub>, H<sub>2</sub>, noble gases, etc.) in situ in the lunar soil at the landing site
- Investigation of organic compounds in the lunar soil
- Measurement of isotope composition of CHON elements (<sup>13</sup>C/<sup>12</sup>C, D/H, <sup>17</sup>O/<sup>16</sup>O, <sup>18</sup>O/<sup>16</sup>O, <sup>15</sup>N/<sup>14</sup>N) and noble gases
- Investigation of the mineralogical composition of the lunar soil, with emphasis on the volatile-bearing minerals using sensor fusion of additional thermal and gas evolving experiments with the use of data from LASMA-LR, and other experiments

To achieve these scientific goals, the GAP complex comprises four modules, the soil preparation and loading system (SDA), the Thermal Differential (Conductivity) Analyzer (TCD), the Gas Chromatograph (GC), and the mass spectrometer (NGMS). Figure 1 shows the schematic flow of the analysis of lunar soil and regolith samples.

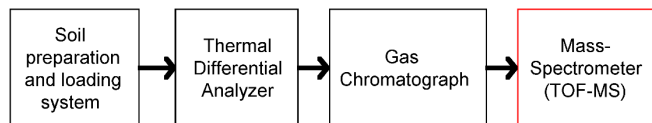


**Figure 1. Block diagram of the GC–MS complex with schematic sample flow.**

While NGMS has two operation modes, the GAP offers multiple configuration options. In NGMS’ GC mode, NGMS will measure mass spectra either of the separated gas exiting the GC column, or it will measure gas directly received from the Thermal Differential Analyzer. In exosphere mode, NGMS will directly analyze the gas from the lunar exosphere.

#### *NGMS as a Standalone Instrument – Lunar Exosphere*

Understanding the lunar exosphere is crucial for comprehending the interactions between the Moon’s surface and its space environment, as well as for future exploration missions. The lunar exosphere is a tenuous atmosphere composed of neutral atoms and molecules released from the surface through processes such as sputtering, thermal

desorption, photo-stimulated desorption, and micrometeoroid impacts [18]–[21]. Despite its tenuous nature, the exosphere holds valuable information about surface composition, solar wind interactions, and the transport of volatiles [22].

The major constituents of the lunar exosphere are hydrogen (H<sub>2</sub>), helium (He), argon (Ar), and water vapor (H<sub>2</sub>O), minor constituents include CHON molecules, krypton (Kr), and xenon (Xe), reference [23]–[25] and references therein. The total number density close to the surface of the Moon is about 10<sup>5</sup> cm<sup>-3</sup>, corresponding to a pressure of about 10<sup>-10</sup> mbar. Analyzing species at number densities of about 1 cm<sup>-3</sup> or even less is desired in the exosphere [24].

By analyzing isotope ratios of noble gases such as helium and argon, NGMS can provide insights into the sources and sinks of exospheric constituents, including contributions from the solar wind, radiogenic decay, and outgassing from the lunar interior [26], [27]. Measurements of transient species like water vapor are vital for assessing the migration of volatiles over the lunar surface and their potential accumulation in cold traps at the lunar poles [20], [28]. These data contribute to our understanding of volatile transport mechanisms and the potential for in situ resource utilization.

## 2. INSTRUMENT ARCHITECTURE

The Neutral Gas Mass Spectrometer (NGMS) is a compact time-of-flight (TOF) [29] mass spectrometer designed for in situ analysis of gaseous samples on the lunar surface. Its design draws heritage from the ROSINA / ROSETTA mass spectrometer [30] but was considerably miniaturized by about a factor of 4 to fit the stringent mass requirements of 3.2 kg. A prototype of this instrument, referred to as P-BACE, was used on a stratospheric balloon mission [31], [32].

Power efficiency is critical due to limited solar power availability at the lunar poles. The NGMS instrument has an allocated maximum primary power consumption of 23 W during nominal operations and less than 6.8 W in standby mode. Nominal operations are provided at 19.0 W, with additional 4.0 W extra for its heaters to maintain the desired GC transfer line temperature. Significant efforts were made to optimize the power consumption of the fast high voltage pulsers and the high-speed data acquisition system. Designing an energy-efficient power system was a major achievement in the development of the NGMS electronics, ensuring the instrument’s functionality within the stringent power constraints of the mission. For comparison, the Neutral Mass Spectrometer (NMS) on board LADEE dissipated 34 W [33].

NGMS operates in two exclusive scientific modes:

- Exosphere mode: NGMS directly measures the gases present in the lunar exosphere from the lander’s location. This mode enables the analysis of

the Moon's tenuous exosphere by analyzing ambient neutral gas.

- GC mode: in this mode, volatiles are extracted from lunar soil samples by heating them in a pyrolysis oven to temperatures up to 1000 °C. The released gases are then either separated by a gas chromatograph prior to analysis or introduced directly into the NGMS for immediate analysis. In both use cases, helium serves as the carrier gas, propelling the sample through a capillary system and into the detector. However, the use of He dilutes the sample, thus posing a sensitivity challenge for NGMS measurements.

A drill unit on the lander collects soil samples from depths up to 1 meter and delivers them to the pyrolysis oven [6]. Upon heating, the released volatiles are transported to the GC unit using helium as a carrier gas. Within the GC, chemical compounds are separated by chemical classes into a time sequence based on their retention times in the GC columns [34]. The GC outputs a continuous flow of carrier gas containing a sequential release of molecules and elements from the sample. Different species exit the GC at different times, corresponding to their specific retention times, with gas chromatographic peak widths on the order of seconds. This temporal separation necessitates a mass spectrometer integration time ranging from 0.1 to 1 seconds to adequately sample the GC output. As the GC delivers a continuous stream of potentially unknown composition, a TOF mass spectrometer is ideal because it acquires the entire mass range (mass-to-charge  $m/z$  1–1000) simultaneously. This approach prevents any loss of sample that can occur with scanning methods, thereby maximizing the sensitivity of the measurement.

#### *GC as the Driver of the Mass Spectrometer Design*

At the time of designing the instrument, the requirement to store a full mass spectrum every 100 ms was a significant design driver. This challenge arose due to the limited write speeds of space grade storage systems, constrained by the performance of readily available space-grade electronic components. The final design includes a double buffering system [35]. Single mass spectra, referred to as waveforms, are recorded at 10 kHz and stored in a short-term buffer (A and B). Then, 1000 (or 10,000) of them are co-added inside this buffer, like a histogram, aligned at the starting signal of the TOF. This data product is referred to as mass spectrum. While buffer A is being used for recording, the content of buffer B is written into a flash memory [35]. Once writing is completed, the buffers swap their purpose. This architecture ensures a sufficient number of sample points per eluent peak in the chromatogram [36], [37]. It is best practice in GC–MS to allow for ideally  $> 7 \dots 11$  points per eluent peak.

Electron ionization facilitates a reliable ionization of the species under analysis. The electrons are provided by two cold-redundant thermionic emitters. The cathode relies on a commercial  $Y_2O_3$ -type disk cathode, which was up-screened,

with typical observed lifetimes in the order of about 5,000 hours at a power consumption of about 1.6 W for the cathode. It heats the ion source to about 250 °C with a time constant of about 2 h. The GC makes direct use of this temperature to avoid condensation of species (see below). The time constant needs to be accounted for in the concept of operations (CONOPS), requiring some conditioning cycle time before operation is stable. Reference [38] describes the effort to develop a space-grade, low-power consumption, durable, robust cathode for spaceflight in detail.

Ion extraction is initiated by a primary pulser (PP). The primary pulser establishes a  $-600$  V extraction field within about 3.2 ns. The subsequent electrostatic acceleration lenses accelerate the ion cloud to the drift energy. Inside the field-free drift tube, the ions separate based on their mass-to-charge ratios along the TOF path. At the end of the drift tube, an ion mirror [39]–[41], referred to as reflectron, and a secondary pulsed electrode are employed.

In GC mode, a secondary pulser (PS) removes selected ions from their path to the detector to prevent detector saturation caused by the ions of the carrier gas without affecting the trajectories of the eluent ions. Typically, the carrier gas (He) is blanked as it dominates the mass spectrum. Ions that are not affected by the PS continue through the second drift region, further separating in time before reaching the detector. Regarding electronics, the secondary pulser is a design copy of the primary pulser, taking advantage of its design, with a minor modification of a slower rise time by modifying the charging resistors, to minimize electronic ringing. Whereas the first pulser consumes about 1.6 W, the second pulser consumes about 1.4 W thanks to the already provided high voltage.

The NGMS ion storage source is specifically designed to address the sensitivity losses inherent to pulsed time-of-flight instruments caused by their duty cycle [42], [43]. In NGMS, single mass spectra (waveforms) are recorded at a 10 kHz rate, while the typical time-of-flight ranges from a few to tens of microseconds. Ideally, the extraction frequency would be on the order of tens of kilohertz, ensuring that the heaviest ions (up to  $m/z$  1000) reach the detector before lighter ions (e.g.,  $m/z$  1) from the subsequent waveform begin arriving. This optimal timing condition is nominally achieved within about 32  $\mu$ s.

However, increasing the extraction frequency beyond 10 kHz is constrained by the thermal limits of the primary pulser's MOSFET. Consequently, NGMS employs an ion storage source, which accumulates ions in the interval between extractions, once the primary pulser recovers and re-establishes a stable electrostatic field (about 2  $\mu$ s after each extraction) until the next extraction event. This design allows the instrument to continuously collect eluting GC gases (or exospheric gases in exosphere mode), significantly boosting overall measurement sensitivity.

Beyond its ion storage capabilities, the NGMS electron ionization source provides a further advantage: the

characteristic fragmentation patterns generated by electron ionization at 70 eV offer additional means of molecular identification. Even though the GC delivers chemical pre-separation of the species, some isobaric interferences may still occur in the mass spectrum, potentially introducing ambiguities in their chemical identification. The distinctive fragment peaks created by electron ionization can appear at a range of masses, thereby helping to distinguish different molecules that share the same nominal mass. Because of the TOF principle, a complete mass spectrum is always recorded, thus all parent and fragment peaks are available for analysis. As a result, the availability of the characteristic fragmentation patterns simplifies data interpretation, enhancing the reliability and clarity of species identification.

### Data Acquisition Electronics

The detection system comprises a high-speed microchannel plate (MCP) detector with an impedance-matched anode [44], capable of resolving ion packets within 500 ps, referred to as pulse width  $\Delta t_{det}$ . Each MCP event generates roughly  $10^6$  electrons per registered ion, resulting in pulse height signals that vary from ion to ion and produce a distribution with a full width at half maximum (FWHM) of about 70 % around the modal gain of  $10^6$ . Ignoring the Gaussian spread in signal amplitude, this gain translates to a current of approximately 3 mA per peak. Across a 50  $\Omega$  load, this corresponds to a voltage of about 150 mV per ion as an order-of-magnitude estimate.

During operation, the detector gain is set such that single-ion peak heights typically range from 10 mV to 100 mV. Consequently, waveform peaks spanning 10 mV to 200 mV are commonly observed, ensuring precise detection and characterization of the ion packets.

A fast detector is essential to analyze higher masses. In fact, all subsystems must be designed for achieving at least unitary mass resolution  $R$  for separation of neighboring peaks, referred to as isobars. The mass resolution is calculated as

$$R = \frac{m}{\Delta m} = \frac{t}{2\Delta t} > 1000 \quad (1)$$

where  $m$  is the mass-per-charge ratio and  $\Delta m$  the peak width measured at FWHM,  $t$  the time-of-flight of a species and  $\Delta t$  the peak width measured in the time spectrum. Many time spreads such as the ion optical resolving power  $\Delta t_{ion}$ , the read-out electronics time spread  $\Delta t_{samples}$ , and the pulse width of the detector  $\Delta t_{det}$  contribute to the total resolving power of the instrument as

$$\Delta t = \sqrt{\sum_i \Delta t_i}. \quad (2)$$

The achieved pulse width of the NGMS detector allows for a mass range of up to about  $m/z$  1000 (see Figure 2, for a mass spectrum with typical mass resolution).

The data acquisition system (DAQ) digitizes the MCP detector output, converting current pulses into voltage peaks.

A 10-bit analog-to-digital converter (ADC) digitizes the pre-amplified signal, using a low noise front-end amplifier. The ADC chip contains two 1 GHz ADCs which can be operated independently or in interleaved mode. The detector signal is split before being pre-amplified with the low noise amplifiers. Each transmission line contains a different gain, resulting in a low and a high gain signal, to increase the dynamic range of the instrument, typically by about 1 order of magnitude. The ADC chip can measure i) interleaved: i-a) measure high gain channel at 10-bit 2 GHz, i-b) measure low gain channel at 10-bit 2 GHz, or ii) measure the high gain channel at 10-bit 1 GHz while measuring the low gain channel at 10-bit 1 GHz (180° phase shift). These three possible configurations allow for a versatile operation.

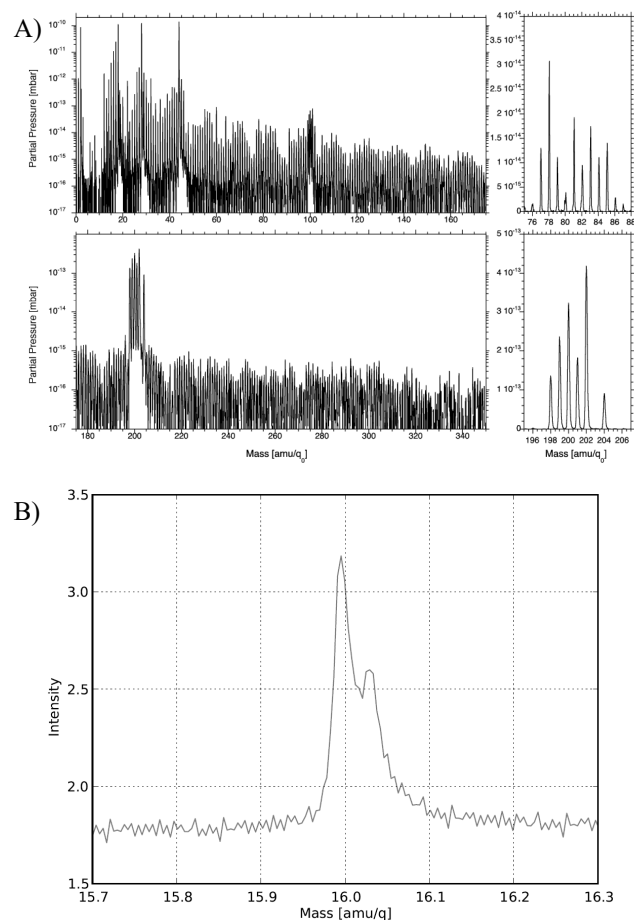


**Figure 2. Mass spectrum of residual gas at a total pressure of  $5.0 \cdot 10^{-10}$  mbar, representing a typical mass spectrum (A). Peaks at nominal  $m/z$  16 can be resolved with the flight-grade hardware (B), attributed to  $\text{CH}_4$  and O.**

Each ion extraction generates a single-shot spectrum or waveform. Summing (co-adding) these waveforms over a defined integration time produces a histogram (time spectrum) that is stored for analysis. The time spectra are recorded in the time domain and are readily converted into mass spectra during data analysis. Due to limited communication opportunities, all mass spectra from a

measurement cycle are stored locally in a ring storage with up to about 8,000 entries until they can be transmitted to Earth, typically once per terrestrial day.

The limited data rate of about 15 Kbyte/s during the main downlink (excluding additional 100 bits/s for housekeeping) required enhanced compression of the spectra, for which we employ a lossy SPIHT compression algorithm [45]. SPIHT has the advantage of filtering noise while compressing as it relies on wavelet transformations. Using this list-free compression algorithm, the compression factor can be chosen to reduce the science data, i.e., to the desired size per spectrum. The science data per spectrum  $d$  are calculated via the effective vertical depth  $v_{eff} d = v_{eff} \cdot h$ , where  $h$  is the horizontal digitization of the instrument, corresponding to the maximum expected flight time, rounded to the next power of 2, as required by the wavelet-type compression algorithm. Typical values are 32 kSamples (low mass mode) or 64 kSamples (high mass mode). The effective vertical depth is calculated as  $v_{eff} = \lceil v + \log_2 N \rceil$ , where  $v$  is the vertical resolution of the ADC (10-bit) and  $N$  the number of commanded co-adds, in the range from 1 to about 2,000,000 (preventing overflow of the memory, about 3 minutes accumulation time). Accepting overflow, which can easily be identified and reverted during post-processing, up to 5 minutes can be co-added. Additional co-adding can be performed during higher-level (ground-based) data analysis.

One advantage of the NGMS electronics architecture is its flexible, parameter-based operation, which functions like an application programming interface (API). By adjusting various parameters, the instrument's state can be reconfigured, and the flight software updates the setup accordingly. This approach proved especially valuable during commissioning, when the final flight parameters had to be determined in situ. It also provides flexibility during lunar operations, such as extending exosphere analysis after surviving the first lunar night or adapting measurement durations based on real-time conditions.

The mission duration on the lunar surface is expected to be at least one lunar day, with the possibility to survive lunar night facilitated by spacecraft survival heaters. Nominal operation temperatures of NGMS range from  $-55\text{ }^{\circ}\text{C}$  to  $+35\text{ }^{\circ}\text{C}$ .



**Figure 3.** PFM, EQM and FS of the drift tube assembly with ceramic-metal ion mirror (top) and ion source (bottom).

### Structure

The NGMS instrument is designed to be highly compact and efficient, with a mass of less than 3.2 kg and envelope dimensions of  $290 \times 176 \times 173\text{ mm}^3$ . Each final flight unit consumed 3.2 kg, including shielding, mounting, and internal harness. The ion optical system itself consumed 647 g, excluding mounting screws and harness. For comparison, NMS on board LADEE consumed 11.8 kg [33].

The lightweight design was enabled by a dedicated manufacturing process of key components of the ion optical system. The brazed metal-ceramic structure enabled a highly compact design of the ion mirror and ion source [40]. Figure 3 shows part of the batch of the flight-grade ion optical hardware. Most of the screws and the mounting supports of more conventional designs were not needed. Figure 4 shows the assembled NGMS ion optical system, including a portion of the exhaust tube (the silver-colored component).

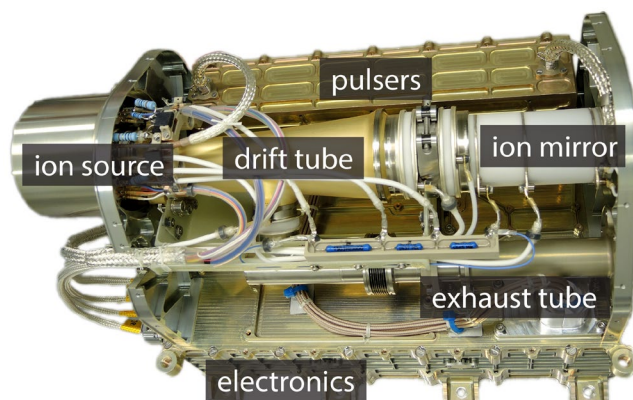


**Figure 4.** NGMS PFM with the protective cover removed. The GC transfer line, which attaches on the left, is not shown in this view.

This design enabled a set of design features, all increasing the performance of the ion optical system. A grid-free ion mirror prevents mass fractionation while increasing the ion optical performance, as the energy focusing is improved given the allocated defined length of the instrument [39]. The opening angle, as defined by the angle between the nominal input and output beam in the ion mirror, could be minimized, as the ion-source structure was small in diameter. In combination with the ultra-compact detector system, this resulted in an opening half-angle only  $1.4^{\circ}$ . In comparison, instruments relying on discrete ion mirrors and ion sources incorporate half-opening angles in the order of 3 to 5 degrees (e.g., reference [46]).

### The GC-MS Interface

The pneumatic coupling between the gas chromatograph and the mass spectrometer is a critical component of any GC-MS system, primarily dictated by throughput requirements. In vacuum technology, throughput  $q_{pr}$  is defined as

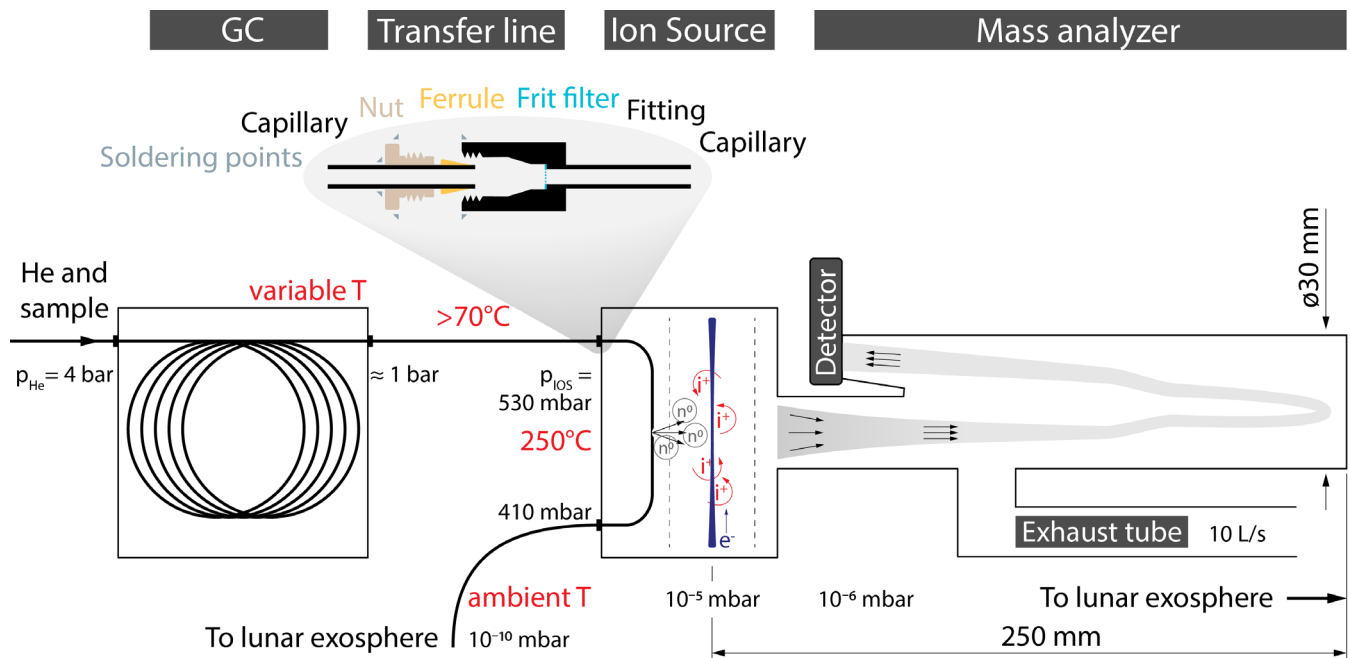


**Figure 5. Schematic overview of the GC–MS interfaces (not to scale). The transfer line is part of the GC subsystem, while the gray boxes represent MS-owned subsystems. Pressure values reflect the expected parameters for the proto-flight model.**

$$q_{pV} = \frac{p \cdot V}{t} = S \cdot p \quad (3)$$

where  $p$  is the pressure at the region of interest,  $V$  is the volume,  $t$  is time, and  $S$  is the volume flow rate, often referred to as pumping speed. This throughput stems from the conductance of the system, which depends on the geometry and flow characteristics of each component. In the viscous flow regime typically employed by GC systems, the throughput remains effectively constant throughout the pneumatic path.

Figure 5 shows the GC–MS coupling schematics. The GC operates with helium at pressures of roughly  $p_{He} = 4$  bar to drive the sample gas through the chromatographic column. At the GC outlet, the pressure is still near 1 bar. Maintaining the integrity of the chromatographic separation requires sustaining a few hundred millibar up to the gas inlet of the ion source ( $p_{IOS}$ ).

Most of the helium carrier gas (including sample gas) flows past the ion source gas inlet and is exhausted through a 1.5 m-long capillary into the lunar environment at approximately  $10^{-10}$  mbar. This capillary is sized to ensure the desired pressure at the ion source inlet, while ensuring the ion source itself remains below about  $10^{-4}$  mbar, thereby keeping the mass spectrometer chamber below  $10^{-5}$  mbar.

An evacuation port of the mass spectrometer, referred to as exhaust tube, ensures a pumping speed of roughly 10 L/s and serves as the entry for exospheric measurements in exosphere mode. Pressure reduction from the GC to the ion source is realized through a  $10 \mu\text{m}$  laser-drilled orifice situated in the

GC line inside the NGMS ion source. This design transforms the GC capillary into a passive split valve. The pressure applied in combination with the  $250 \mu\text{m}$  inner diameter of the capillary results in a laminar flow at the split interface. Such laminar conditions mitigate mass (including isotope) fractionation and reduce GC peak broadening caused by turbulent mixing. By restricting the flow into the ion source, the orifice preserves the pressure conditions required for stable operation of the mass spectrometer and upholds the integrity of the GC separation.

It is well-established that certain chemical compounds are prone to condensation within the GC transfer line, potentially preventing them from reaching the mass spectrometer and compromising measurements. To address this issue, the transfer line is actively heated to at least  $70^\circ\text{C}$ , ensuring that volatile species remain in the gas phase. Moreover, the ion source operates at approximately  $250^\circ\text{C}$ , creating a monotonically increasing temperature gradient as the gas travels from the GC toward the split valve region.

Because temperature gradients can lead to flow inhomogeneities, the GC transfer line is mechanically isolated, with no additional connections other than its mounting points at the GC and the MS. By minimizing thermal contact along its length, the design maintains a stable temperature profile. After the split valve, the capillary cools back down to the ambient spacecraft temperature, preventing excessive heating of surrounding components while still preserving the integrity of the chromatographic analysis.

The orifice diameter is a key parameter for ensuring proper coupling between the GC and the MS. It must be sufficiently

small to maintain low pressure in the ion source. Excessive pressure can violate two primary conditions for optimal MS operation: (1) the mean free path of ions must remain on the order of tens to hundreds of kilometers, minimizing collisions within the mass analyzer and thereby preventing ion-molecule reactions in the ion source, and (2) the detector must operate at pressures below  $10^{-5}$  mbar.

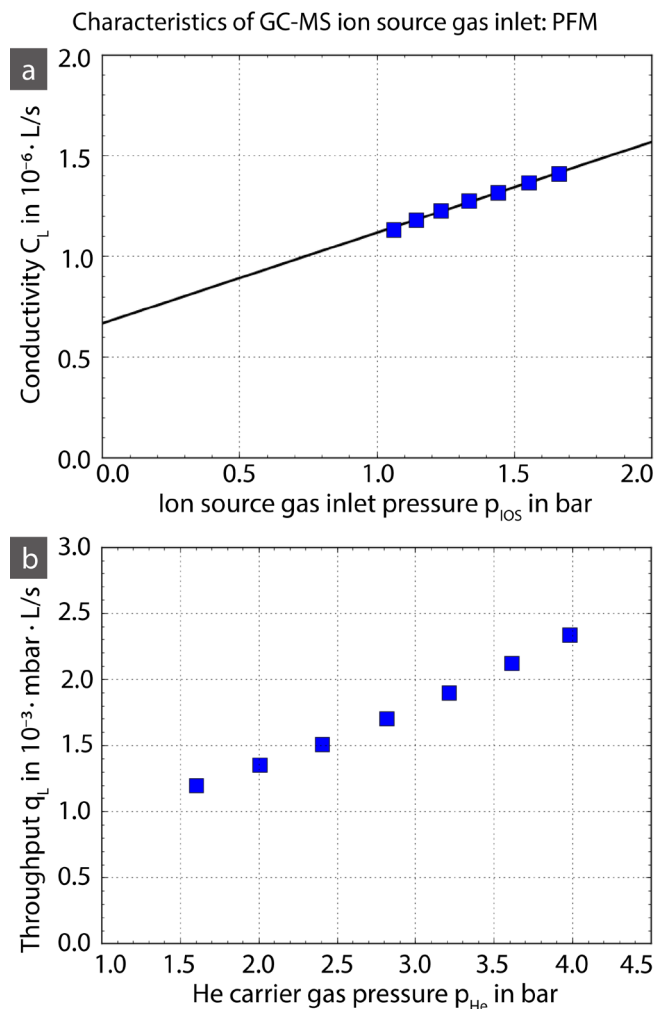


**Figure 6. The measured conductivity of the gas inlet within the ion source remains sufficiently linear across the operation range of the helium carrier gas (a). Because of the minimal variance, error bars are not visible. The resulting throughput is large enough to enable sensitive analyses while maintaining the required vacuum conditions in the ion source.**

An orifice-based split valve was selected for its simplicity under flight conditions. This orifice required a dedicated manufacturing campaign, during which different manufacturing parameters were explored until a satisfactory configuration was identified. Laser drilling proved suitable for achieving the required diameter but resulted in considerable effort in development and testing. Figure 6 illustrates the pressure–conductance relationship determined during split valve testing of the proto-flight model (PFM) component.

A significant challenge is preventing clogging in the micrometer-scale orifice. To address this issue, 1/32-inch,  $0.5 \mu\text{m}$  frit filters were installed at both the inlet and outlet of the GC interface at the MS. Achieving ultrahigh vacuum-compatible seals also posed difficulties. In prototype configurations, stainless steel fittings with Polyimide Valcon ferrules (Valco Instruments Co. Inc., USA) were used. For the PFM, the transfer line was designed as expendable, and the ferrules were manufactured from gold-plated steel. After tightening, the nut–capillary–fitting junction is brazed with a silver–tin alloy, ensuring a leak-tight and secure seal. These design choices ultimately yield a robust GC–MS interface for spaceflight suitable for high-sensitivity gas analyses.

### 3. SCIENTIFIC PERFORMANCE

NGMS demonstrated its scientific excellence over many verification steps. As the Luna program included projects on diverse level of maturation, NGMS’ scientific assessment needed to rely on data from both prototype and flight instruments.

#### *Exosphere Mode*

The first prototypes built for NGMS were the EGT [47] and the P-BACE instruments [31]. They were ion optically identical as NGMS later but operated with laboratory electronics. Figure 2 demonstrates that the NGMS ion optical system can resolve the mass peaks at  $m/z$  84, attributed to krypton, as assessed by EGT. There, the mass resolution is about 1200 (FWHM) and about constant for higher masses. The mass spectrum is clipped at  $m/z$  350 for clarity reasons only, but would continue to about  $m/z$  1000, limited by the resolving power of the ion optical system, Equation 2, and by the allocated memory size and data transmission budget. For an analysis of species present in the lunar exosphere [24] (and regolith), this mass range allows to detect even species with unlikely high mass.

Such species typically occur only in trace amounts. Hence, a high dynamic range is required. The mass spectrum shows the achieved instantaneous dynamic range by this system, about six orders of magnitude within 1 s accumulation time, i.e., 10,000 co-added waveforms, thanks to the stability of the instrument. This dynamic range is enabled by a design transmission of the ion optical system of 1, as modeled in SIMION, an ion optical simulation software. The nominal ion optical transmission of 1 also translates to a high sensitivity and prevents mass fractionation, which is critical for accurate isotope measurements. In addition, the dynamic range can be expanded by varying the electron emission current in the ion source ( $10\text{--}300 \mu\text{A}$ ) and adjusting the detector gain. Overall, a dynamic range of about 10 decades can be achieved.

Considering the residual gas pressure during the measurement, which was in the order of magnitude of the surface pressure of the Moon, the counts (per second) can be calibrated to achieve the partial pressures of the species. Species with a partial pressure in the order of  $10^{-16}$  mbar can

be analyzed, within 1 s. Similar results were observed with the next generation of prototype and the flight instrument, where mass resolutions exceeding 1000 were achieved [35]. This pressure range corresponds to a number density range of about 1 to  $10^6 \text{ cm}^{-3}$ . The measurements can be prolonged and further mass spectra can be co-added. In principle, co-adding is possible over extended durations, even terrestrial days, as shown during a flight of P-BACE [32].

#### GC Mode

The flight-grade gas chromatograph has not been available at the time of writing this article. Studies were conducted on prototype versions of both the GC and the NGMS initially, and later confirmed with more evolved GC columns and a fully flight-representative NGMS ion optical system [34], [36], [37], [48].

**Table 1. Target list of gases for GAP. PAH: Polycyclic aromatic hydrocarbons. References provided in the text.**

Column	CP-Molsieve 5Å	PoraPLOT Q
<b>Main group</b>	H <sub>2</sub> , CO, CH <sub>4</sub>	H <sub>2</sub> O, CO <sub>2</sub> , SO <sub>2</sub> , H <sub>2</sub> S, COS, CS <sub>2</sub> , C <sub>2</sub> – C <sub>6</sub>
<b>Accessory group</b>	NO <sub>x</sub> , N <sub>2</sub>	HCN, CH <sub>3</sub> CHO, C <sub>10</sub> H <sub>8</sub> (+PAH)
<b>Occasional group</b>	O <sub>2</sub> , Kr, Xe, Ar, Ne, He	

Table 1 shows the two foreseen flight GC columns and their chemical target groups to investigate the lunar volatiles and mineralogy. However, during prototype testing, the organic compounds were analyzed with the MXT-5 column and noble gases with the Carbobond column. Due to the high sensitivity and the large dynamic range, NGMS is able to detect species at very low concentrations, far below the detection limit of the thermal conductivity detector (TCD). For NGMS, we determined the detection limit as 10 pmol [36]. For a regolith sample volume of about 500 mm<sup>3</sup>, we estimate for the detection limit in the regolith as low as  $2 \cdot 10^{-10}$  by mass for hydrocarbons. For comparison, for the SAM instrument, the GC-MS on the Curiosity rover of NASA, the reported sensitivity for organic compounds is  $6 \cdot 10^{-10}$  by mass [49]. The detection limits of noble gases are estimated at  $2 \cdot 10^{-9}$  by mass [36].

We obtained similar GC-MS results when using the flight-grade NGMS (engineering qualification model EQM), however, the detection limit for noble gases was improved for the EQM ion optical system, with detection limits of the hydrocarbon of about  $2 \cdot 10^{-11}$  by mass and  $2 \cdot 10^{-10}$  by mass for the noble gases krypton and xenon. To conclude on the final detection limits, the flight-grade GC would be required. Hence, we consider the conservative prototype results as upper limits.

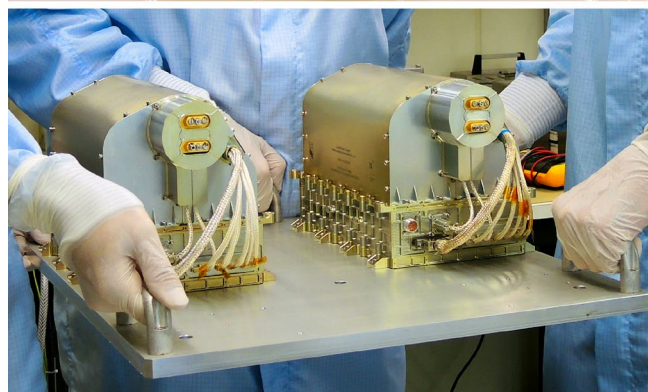
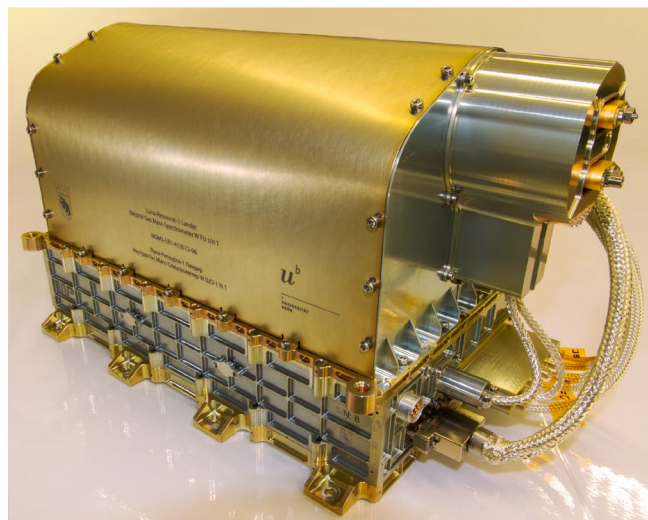


**Figure 7. Flight unit of the NGMS instrument (upper panel) with flight spare during cross-calibration (lower panel). Notice the hands for scale.**

## 4. STATUS

The NGMS instrument underwent a rigorous qualification process, including an EQM, a PFM, and a Flight Spare (FS). The two fully qualified instruments, PFM and FS, reached technology readiness level (TRL) 8, making them flight-ready. Following the European Space Agency's withdrawal from the Luna program, efforts were made to repurpose these instruments for other missions, primarily in exosphere mode. A subsequent investigation considered integrating key NGMS components into the CODEX mass spectrometer [50] on board NASA's DIMPLE payload. However, detailed assessments revealed that the modifications required to meet DIMPLE's specifications were too extensive, mainly due to different structure requirements and more modern communication interfaces. As a result, both the Luna NGMS project and attempts to integrate the instrument into alternative missions were ultimately discontinued.

## 5. IMPACT

The NGMS instrument has served as the foundational baseline for three mass spectrometers selected for spaceflight thus far: the Neutral and Ion Mass Spectrometer (NIM) on board ESA's JUICE mission [51], MANIaC on board ESA's Comet Interceptor mission [46], and CODEX on board NASA's DIMPLe payload [50]. Its laboratory prototypes continue to be used for analyzing noble gases from meteorites [47].

Two re-builds of NGMS with commercial components were manufactured and used for prototyping and to study the behavior of irradiated ice samples in situ [52], demonstrating its ongoing relevance in scientific research. Additionally, NGMS serves as the baseline mass spectrometer design for other future mission such as the, for example, possible Uranus atmospheric probe as part of the Uranus Orbiter and probe mission [53]. Recent conceptual designs for mass spectrometers intended for spacecraft flybys at high relative encounter velocities also rely on the NGMS architecture [54]. The development of NGMS has significantly contributed to academic advancement, culminating in three PhD theses and one BSc thesis directly linked to its hardware development.

In addition to its impact on space exploration, the NGMS instrument was commercialized through a university spin-off venture, Spacetek Technology AG, Gümligen, Switzerland. While the commercial version was optimized for analyzing plasma processes in the semiconductor industry, it retained the fundamental architecture of NGMS. This underscores the instrument's versatility and the robustness of its design, allowing it to be adapted for various applications far beyond its original scope.

## 6. SUMMARY

The Neutral Gas Mass Spectrometer (NGMS) is a pioneering compact time-of-flight mass spectrometer designed to analyze the element, isotope, and molecular composition of the lunar regolith and exosphere, including essential CHON compounds (carbon, hydrogen, oxygen, nitrogen), water, and noble gases. By integrating seamlessly with a gas chromatograph and a pyrolysis oven, NGMS enables comprehensive analysis of volatile species, providing profound insights into the processes that have shaped the lunar surface.

The innovative architecture of NGMS led to a design that outperforms comparable instruments across most, if not all, relevant assessment criteria. It has revolutionized the portfolio of compact spaceborne mass spectrometers, serving as an architectural baseline for many subsequent instruments. The NGMS design allows for detailed analysis of the surface and exosphere of the Moon and potentially even beyond, significantly advancing our ability to investigate the origin and evolution of the Solar System.

## LIST OF ABBREVIATIONS, ACRONYMS, AND SYMBOLS

ADC	Analogue to Digital Converter
API	Application Programming Interface
CODEX	Chemistry, Organics, and Dating Experiment
CONOPS	CONcept of OPERationS
DAQ	Data AcQuisition system
DIMPLe	Dating an Irregular Mare Patch with a Lunar Explorer
EGT	EdelGasTof
EQM	Engineering Qualification Model
ESA	European Space Agency
FS	Flight Spare model
FWHM	Full Width at Half Maximum
GAP	Gas Analytical Package
GC	Gas Chromatograph
GC-MS	Gas Chromatograph Mass Spectrometry / Spectrometer
ISRO	Indian Space Research Organisation
ISRU	In Situ Resource Utilization
JUICE	JUpiter ICy moon Explorer
LADEE	Lunar Atmosphere and Dust Environment Explorer
LASMA	LASer ablation MAss spectrometer
LCROSS	Lunar CRater Observation and Sensing Satellite
LRO	Lunar Reconnaissance Orbiter
m	Mass
$\Delta m$	Peak width of the mass of interest, measured as FWHM
m/z	Mass per charge ratio
m/ $\Delta m$	Mass resolution
M <sup>3</sup>	Moon Mineralogy Mapper
MANIaC	Mass Analyzer for Neutrals and Ions at Comets
MOSFET	Metal-Oxide-Semiconductor Field-Effect Transistor
NASA	National Aeronautics and Space Administration
NGMS	Neutral Gas Mass Spectrometer
NIM	Neutral and Ion Mass spectrometer
NMS	Neutral Mass Spectrometer
p	Pressure
PAH	Polycyclic Aromatic Hydrocarbons
P-BACE	Polar Balloon Atmospheric Composition Experiment
PFM	Proto-Flight Model
PP	Primary Pulser
PS	Secondary Pulser
R	Mass resolution
ROSETTA	Name
ROSINA	Rosetta Orbiter Spectrometer for Ion and Neutral Analysis
SAM	Sample Analysis at Mars
SIMION	Commercial software for simulation of trajectories of charged particles
SPIHT	Set Partitioning In Hierarchical Trees
t	Time-of-flight
$\Delta t$	Peak width of the peak of interest, measured as FWHM
TCD	Thermal Conductivity Detector
TOF	Time-Of-Flight
TOF-MS	Time-Of-Flight Mass Spectrometer
TRL	Technical Readiness Level

## ACKNOWLEDGEMENTS

The financial support by the Swiss National Science Foundation and the Swiss Space Office are gratefully acknowledged. We sincerely thank all staff involved in this activity. We declare no conflict of interests.

## REFERENCES

- [1] I. Mitrofanov and L. Zelenyi, "Lunar Landers of Luna-Glob and Luna-Resource missions: science goals and instrumentation," in *EGU 2013*, 2013, p. 8517.
- [2] V. V. Khartov, L. M. Zelenyi, V. P. Dolgoplov, V. V. Efanov, O. N. Zaytseva, A. V. Lukiyanchikov, M. B. Martynov, and K. M. Pichkhadze, "New Russian lunar unmanned space complexes," *Solar System Research*, vol. 45, no. 7, pp. 690–696, Dec. 2011, doi: 10.1134/S0038094611070100.
- [3] A. E. Chumikov, V. S. Cheptsov, P. Wurz, D. Lasi, J. Jost, and N. G. Managadze, "Design, characteristics and scientific tasks of the LASMA-LR laser ionization mass spectrometer onboard Luna-25 and Luna-27 space missions," *Int J Mass Spectrom*, vol. 469, p. 116676, 2021, doi: 10.1016/j.ijms.2021.116676.
- [4] O. I. Turchinskaya and E. N. Slyuta, "Landing site choice for Luna-27 mission in the Moon South Polar Region," *Acta Astronaut*, vol. 222, pp. 346–358, Sep. 2024, doi: 10.1016/j.actaastro.2024.06.011.
- [5] A. B. Sanin *et al.*, "Hydrogen distribution in the lunar polar regions," *Icarus*, vol. 283, pp. 20–30, Feb. 2017, doi: 10.1016/j.icarus.2016.06.002.
- [6] R. Trautner *et al.*, "PROSPECT: A comprehensive sample acquisition and analysis package for lunar science and exploration," *Frontiers in Space Technologies*, vol. 5, Apr. 2024, doi: 10.3389/frspt.2024.1331828.
- [7] I. Mitrofanov, "Update on Luna 25 and Luna 27 Polar Landers," in *EGU General Assembly 2019*, Geophysical Research Abstracts, 2019.
- [8] I. A. Crawford, "Lunar resources: A review," *Prog Phys Geogr*, vol. 39, pp. 137–167, 2015, doi: 10.1177/0309133314567585.
- [9] M. Anand, I. A. Crawford, M. Balat-Pichelin, S. Abanades, W. Van Westrenen, G. Péraudeau, R. Jaumann, and W. Seboldt, "A brief review of chemical and mineralogical resources on the Moon and likely initial in situ resource utilization (ISRU) applications," in *Planetary and Space Science*, Dec. 2012, pp. 42–48. doi: 10.1016/j.pss.2012.08.012.
- [10] S. R. Taylor, "Earth-Moon System, Planetary Science, and Lessons Learned," *Rev Mineral Geochem*, vol. 60, no. 1, pp. 657–704, Jan. 2006, doi: 10.2138/rmg.2006.60.7.
- [11] W. C. Feldman, "Fluxes of Fast and Epithermal Neutrons from Lunar Prospector: Evidence for Water Ice at the Lunar Poles," *Science (1979)*, vol. 281, no. 5382, pp. 1496–1500, Sep. 1998, doi: 10.1126/science.281.5382.1496.
- [12] A. Colaprete, P. Schultz, J. Heldmann, D. Wooden, M. Shirley, K. Ennico, B. Hermalyn, W. Marshall, A. Ricco, R. C. Elphic, D. Goldstein, D. Summy, G. D. Bart, E. Asphaug, D. Korycansky, D. Landis, and L. Sollitt, "Detection of Water in the LCROSS Ejecta Plume," *Science (1979)*, vol. 330, no. 6003, pp. 463–468, Oct. 2010, doi: 10.1126/science.1186986.
- [13] C. M. Pieters *et al.*, "The Moon mineralogy mapper (M3) on Chandrayaan-1," *Curr Sci*, vol. 96, no. 4, pp. 500–505, 2009.
- [14] R. N. Clark, "Detection of Adsorbed Water and Hydroxyl on the Moon," *Science (1979)*, vol. 326, no. 5952, pp. 562–564, Oct. 2009, doi: 10.1126/science.1178105.
- [15] A. E. Saal, E. H. Hauri, M. Lo Cascio, J. A. Van Orman, M. C. Rutherford, and R. F. Cooper, "Volatile content of lunar volcanic glasses and the presence of water in the Moon's interior," *Nature*, vol. 454, no. 7201, pp. 192–195, Jul. 2008, doi: 10.1038/nature07047.
- [16] G. B. Sanders and W. E. Larson, "Final review of analog field campaigns for In Situ Resource Utilization technology and capability maturation," *Advances in Space Research*, vol. 55, no. 10, pp. 2381–2404, May 2015, doi: 10.1016/j.asr.2014.12.024.
- [17] M. V. Gerasimov *et al.*, "Gas-Analytic Package for the Russian Luna-Globe and Lunar-Resource missions," in *EPSC-DPS2011*, 2011, pp. 1–2.
- [18] P. Wurz, U. Rohner, J. A. Whitby, C. Kolb, H. Lammer, P. Dobnikar, and J. A. Martín-Fernández, "The lunar exosphere: The sputtering contribution," *Icarus*, vol. 191, no. 2, pp. 486–496, 2007, doi: 10.1016/j.icarus.2007.04.034.
- [19] M. Benna, P. R. Mahaffy, J. S. Halekas, R. C. Elphic, and G. T. Delory, "Variability of helium, neon, and argon in the lunar exosphere as observed by the LADEE NMS instrument," *Geophys Res Lett*, vol. 42, no. 10, pp. 3723–3729, May 2015, doi: 10.1002/2015GL064120.
- [20] D. M. Hurley, J. C. Cook, K. D. Retherford, T. Greathouse, G. R. Gladstone, K. Mandt, C. Grava, D. Kaufmann, A. Hendrix, P. D. Feldman, W. Pryor, A. Stickle, R. M. Killen, and S. A. Stern, "Contributions of solar wind and micrometeoroids to molecular hydrogen in the lunar exosphere," *Icarus*, vol. 283, pp. 31–37, Feb. 2017, doi: 10.1016/j.icarus.2016.04.019.
- [21] P. Wurz, S. Fatemi, A. Galli, J. Halekas, Y. Harada, N. Jäggi, J. Jasinski, H. Lammer, S. Lindsay, M. N. Nishino, T. M. Orlando, J. M. Raines, M. Scherf, J. Slavin, A. Vorburger, and R. Winslow, "Particles and Photons as Drivers for Particle Release from the Surfaces of the Moon and Mercury," *Space Sci Rev*, vol. 218, no. 3, p. 10, Apr. 2022, doi: 10.1007/s11214-022-00875-6.
- [22] P. Lucey, "Understanding the Lunar Surface and Space-Moon Interactions," *Rev Mineral Geochem*, vol. 60, no. 1, pp. 83–219, Jan. 2006, doi: 10.2138/rmg.2006.60.2.
- [23] J. C. Cook, S. A. Stern, P. D. Feldman, G. R. Gladstone, K. D. Retherford, and C. C. C. Tsang, "New upper limits on numerous atmospheric species in the native lunar atmosphere," *Icarus*, vol. 225, no. 1, pp. 681–687, Jul. 2013, doi:

- 10.1016/j.icarus.2013.04.010.
- [24] P. Wurz, D. Abplanalp, M. Tulej, and H. Lammer, "A neutral gas mass spectrometer for the investigation of lunar volatiles," *Planet Space Sci*, vol. 74, no. 1, pp. 264–269, Dec. 2012, doi: 10.1016/j.pss.2012.05.016.
- [25] S. A. Stern, "The lunar atmosphere: History, status, current problems, and context," *Reviews of Geophysics*, vol. 37, no. 4, pp. 453–491, Nov. 1999, doi: 10.1029/1999RG900005.
- [26] J. H. Hoffman and R. R. Hodges, "Molecular gas species in the lunar atmosphere," *The Moon*, vol. 14, no. 1, pp. 159–167, Sep. 1975, doi: 10.1007/BF00562981.
- [27] M. Benna, D. M. Hurley, T. J. Stubbs, P. R. Mahaffy, and R. C. Elphic, "Lunar soil hydration constrained by exospheric water liberated by meteoroid impacts," *Nat Geosci*, vol. 12, no. 5, pp. 333–338, May 2019, doi: 10.1038/s41561-019-0345-3.
- [28] D. H. Crider and R. R. Vondrak, "Hydrogen migration to the lunar poles by solar wind bombardment of the Moon," *Advances in Space Research*, vol. 30, no. 8, pp. 1869–1874, Oct. 2002, doi: 10.1016/S0273-1177(02)00493-3.
- [29] W. C. Wiley and I. H. McLaren, "Time-of-Flight Mass Spectrometer with Improved Resolution," *Review of Scientific Instruments*, vol. 26, no. 12, pp. 1150–1157, Dec. 1955, doi: 10.1063/1.1715212.
- [30] H. Balsiger *et al.*, "Rosina – Rosetta Orbiter Spectrometer for Ion and Neutral Analysis," *Space Sci Rev*, vol. 128, no. 1–4, pp. 745–801, May 2007, doi: 10.1007/s11214-006-8335-3.
- [31] D. Abplanalp, P. Wurz, L. Huber, I. Leya, E. Kopp, U. Rohner, M. Wieser, L. Kalla, and S. Barabash, "A neutral gas mass spectrometer to measure the chemical composition of the stratosphere," *Advances in Space Research*, vol. 44, no. 7, pp. 870–878, Oct. 2009, doi: 10.1016/j.asr.2009.06.016.
- [32] P. Wurz, D. Abplanalp, M. Tulej, M. Iakovleva, V. A. Fernandes, A. Chumikov, and G. G. Managadze, "Mass spectrometric analysis in planetary science: Investigation of the surface and the atmosphere," *Solar System Research*, vol. 46, no. 6, pp. 408–422, Nov. 2012, doi: 10.1134/S003809461206007X.
- [33] R. C. Elphic and C. T. Russell, *The Lunar Atmosphere and Dust Environment Explorer Mission (LADEE)*. Cham: Springer International Publishing, 2015. doi: 10.1007/978-3-319-18717-4.
- [34] D. Coscia, C. Szopa, M. Gerasimov, P. Wurz, L. Hofer, M. Cabane, P. Coll, A. Buch, R. Fausch, A. Sapgir, S. Aseev, and M. A. Zaitsev, "In Situ Analysis of the Volatiles in the Lunar Regolith with the Gas Analytical Package Experiment: Calibration of a GCMS Prototype," in *American Astronomical Society*, Pasadena, California, USA, Oct. 2016.
- [35] R. G. Fausch, P. Wurz, M. Tulej, J. Jost, P. Gubler, M. Gruber, D. Lasi, C. Zimmermann, and T. Gerber, "Flight electronics of GC-mass spectrometer for investigation of volatiles in the lunar regolith," *2018 IEEE Aerospace Conference*, pp. 1–13, 2018, doi: 10.1109/AERO.2018.8396788.
- [36] L. Hofer, P. Wurz, A. Buch, M. Cabane, P. Coll, D. Coscia, M. Gerasimov, D. Lasi, A. Sapgir, C. Szopa, and M. Tulej, "Prototype of the gas chromatograph–mass spectrometer to investigate volatile species in the lunar soil for the Luna-Resurs mission," *Planet Space Sci*, vol. 111, no. 1, pp. 126–133, Jun. 2015, doi: 10.1016/j.pss.2015.03.027.
- [37] C. Szopa, M. Gerasimov, P. Wurz, R. Fausch, A. Buch, M. Cabane, P. Coll, D. Coscia, L. Hofer, D. Lasi, A. Sapgir, M. Tulej, and M. Zaitsev, "In Situ Pyro-GCMS Chemical Analysis of Lunar Soil with the Gas Analytical Complex Experiment of the Future Luna-Resurs Mission," in *42nd COSPAR Scientific Assembly*, Pasadena, California, USA, Jul. 2018.
- [38] R. Fausch, M. Föhn, L. Hofer, S. Meyer, P. Wahlström, S. S. Wyler, and P. Wurz, "Power-Efficient Electron Emitters for Electron Ionization in Spaceborne Mass Spectrometers," in *2024 IEEE Aerospace Conference*, IEEE, Mar. 2024, pp. 1–19. doi: 10.1109/AERO58975.2024.10521278.
- [39] S. Scherer, K. Altwegg, H. Balsiger, J. Fischer, A. Jäckel, A. Korth, M. Mildner, D. Piazza, H. Reme, and P. Wurz, "A novel principle for an ion mirror design in time-of-flight mass spectrometry," *Int J Mass Spectrom*, vol. 251, no. 1, pp. 73–81, Mar. 2006, doi: 10.1016/j.ijms.2006.01.025.
- [40] H. R. Elsener, B. Rheingangs, L. P. H. Jeurgens, T. Burgdorf, S. Brüngger, D. Piazza, and P. Wurz, "Brazed metal-ceramic components for space applications," in *Lectures and Posters of the 12th International Conference on Brazing, High Temperature Brazing and Diffusion Bonding*, Düsseldorf, Germany: DVS-Berichte Band 353, 2019. Accessed: Oct. 31, 2023. [Online]. Available: <https://boris.unibe.ch/153270/>
- [41] B. Mamyrin, V. Karataev, D. Shmikk, and V. Zagulin, "The mass-reflectron, a new nonmagnetic time-of-flight mass spectrometer with high resolution," *Soviet Journal of Experimental and Theoretical Physics*, vol. 37, no. 1, p. 45, 1973.
- [42] R. Grix, U. Grüner, G. Li, H. Stroh, and H. Wollnik, "An electron impact storage ion source for time-of-flight mass spectrometers," *Int J Mass Spectrom Ion Process*, vol. 93, no. 3, pp. 323–330, Oct. 1989, doi: 10.1016/0168-1176(89)80121-1.
- [43] D. Abplanalp, P. Wurz, L. Huber, and I. Leya, "An optimised compact electron impact ion storage source for a time-of-flight mass spectrometer," *Int J Mass Spectrom*, vol. 294, no. 1, pp. 33–39, Jun. 2010, doi: 10.1016/j.ijms.2010.05.001.
- [44] P. Wurz and L. Gubler, "Impedance-matching anode for fast timing signals," *Review of Scientific Instruments*, vol. 65, no. 4, pp. 871–876, 1994, doi: 10.1063/1.1144914.
- [45] F. W. Wheeler and W. A. Pearlman, "SPIHT image compression without lists," in *2000 IEEE*

*International Conference on Acoustics, Speech, and Signal Processing. Proceedings (Cat. No.00CH37100)*, IEEE, 2000, pp. 2047–2050. doi: 10.1109/ICASSP.2000.859236.

- [46] C. Snodgrass and G. H. Jones, “The European Space Agency’s Comet Interceptor lies in wait,” *Nat Commun*, vol. 10, no. 1, pp. 1–4, 2019, doi: 10.1038/s41467-019-13470-1.
- [47] A. Riedo, S. Rout, R. Wiesendanger, P. Wurz, and I. Leya, “EGT—A sensitive time-of-flight mass spectrometer for multielement isotope gas analysis,” *Journal of Mass Spectrometry*, vol. 53, no. 11, pp. 1036–1045, Nov. 2018, doi: 10.1002/jms.4275.
- [48] S. A. Aseev, M. V. Gerasimov, M. A. Zaitsev, and A. G. Sapgir, “Analysis of volatile lunar compounds: The study of gas retention time on Carbosieve SIII adsorbent with respect to temperature,” *Cosmic Research*, vol. 54, no. 5, pp. 358–365, 2016, doi: 10.1134/S0010952516050026.
- [49] P. R. Mahaffy *et al.*, “The sample analysis at Mars investigation and instrument suite,” *Space Sci Rev*, vol. 170, no. 1–4, pp. 401–478, 2012, doi: 10.1007/s11214-012-9879-z.
- [50] J. Levine, F. Scott Anderson, S. Braden, R. G. Fausch, S. Foster, G. Fowler, K. H. Joy, S. Osterman, J. Pernet-Fisher, S. Seddio, T. Whitaker, P. Wurz, M. Yant, and T. Ee Yap, “Dating Granites Using CODEX, with Application to In Situ Dating on the Moon,” *Planet Sci J*, vol. 4, no. 5, May 2023, doi: 10.3847/PSJ/accd6c.
- [51] M. Föhn, A. Galli, A. Vorburger, M. Tulej, D. Lasi, A. Riedo, R. G. Fausch, M. Althaus, S. Brungger, P. Fahrer, M. Gerber, M. Luthi, H. P. Munz, S. Oeschger, D. Piazza, and P. Wurz, “Description of the Mass Spectrometer for the Jupiter Icy Moons Explorer Mission,” *2021 IEEE Aerospace Conference*, pp. 1–14, Mar. 2021, doi: 10.1109/AERO50100.2021.9438344.
- [52] C. Tinner, A. Galli, F. Bär, A. Pommerol, M. Rubin, A. Vorburger, and P. Wurz, “Electron-induced radiolysis of water ice and the buildup of O,” in *EGU 2023*, Vienna, Apr. 2023. doi: 10.5194/egusphere-egu23-7540.
- [53] A. Vorburger, P. Wurz, R. Helled, and O. Mousis, “Mass Spectrometer Experiment for a Uranus Probe,” *Space Sci Rev*, vol. 220, no. 6, p. 64, Sep. 2024, doi: 10.1007/s11214-024-01096-9.
- [54] R. G. Fausch, J. A. Schertenleib, and P. Wurz, “Advances in Mass Spectrometers for Flyby Space Missions for the Analysis of Biosignatures and Other Complex Molecules,” *Universe*, vol. 8, no. 8, p. 416, Aug. 2022, doi: 10.3390/universe8080416.

## BIOGRAPHY



**Rico G. Fausch** completed an apprenticeship as a mechanical design engineer before he received a B.Sc. in Systems Engineering (micro technologies) from NTB University of Applied Science (Switzerland) in 2013 and an M.Sc. in Biomedical Engineering from University of Bern (Switzerland) in 2015. He has been with the Physics Institute of the University of Bern since 2016, where he received his Ph.D. in Physics in 2020 for the development of the flight units of NGMS / Luna 27. As a researcher and project manager, he is involved in the design of several space missions and space instrumentation including NGMS / Luna 27, LASMA / Luna 25 and 27, NIM / PEP / JUICE (ESA), CubeSatTOF / CHESS, and CODEX / DIMPLE / CLPS (NASA).



**Hans Rudolf Elsener** received his master’s and Ph.D. degree in Chemistry from ETH Zurich in 1991. He began his career as a development and process engineer at AFIF. In 1997, he joined Empa in Zurich as a development and process engineer. Since 2002, he has been a development engineer at Empa in Dübendorf. He specializes in developing advanced materials and processes, contributing significantly to both scientific research and industrial applications. He is involved in the design manufacturing of many mass spectrometers for deep space missions, including the NGMS on board the Luna missions.



**Lukas Hofer** received an M.Sc. in physics from the University of Bern in 2011, and a Ph.D. in 2015 for the development of the NGMS instrument on board the Luna 27 mission. He is now CSO and Co-founder at a startup, where he is responsible for the development of commercial mass spectrometers.



**Jürg Jost** received a B.Sc. in Electrical Engineering and a M.Sc. in Automation Engineering from Bern University of Applied Sciences (Switzerland) in 1997 and 2003. Since 2001 he leads the electronics group of the Space Research & Planetary Sciences Department, University of Bern. He managed, designed, built, qualified and delivered many electronic parts and

systems for previous and present space missions like Rosina / ROSETTA, PLASTIC / STEREO, IBEX, P-BACE / MEAP, BELA, ENA and STROFIO / BepiColombo, LASMA / Phobos-Grunt, LASMA-L and NGMS / Luna 25 and 27, NIM / PEP / JUICE, CaSSIS / Exo-Mars, CHEOPS. He is now CTO and Co-founder at a startup, where he is responsible for the technology of mass spectrometers.



**Davide Lasi** received a B.Sc. and an M.Sc. in Chemistry from the University of Milano in 2004 and 2006, and an M.S. from MIT in 2018 (System Design and Management). He has been with the University of Bern (2011–2021) as project manager for NGMS / Luna 27, LASMA / Luna 25 and 27, NIM / PEP / JUICE (ESA). He currently works at the

AWS Center for Quantum Computing.



**Daniele Piazza** has more than 20 years of experience in the design and development of space instruments. He has a Ph.D. in mechanical engineering from ETH Zurich and started his career in Formula 1. Since 2005 he has been leading the mechanical engineering group working on space instruments at the University of Bern, Switzerland.



**Peter Wurz** has a degree in electronic engineering (1985), an M.Sc. and a Ph.D. in Physics from Technical University of Vienna, Austria (1990). He has been a post-doctoral researcher at Argonne National Laboratory, USA. Since 1992 at the University of Bern. He is Professor of physics, 2015–2022 head of the Space Science and

Planetology division, and since 2022 director of the physics institute. He has been Co-I and PI for many science instruments for space missions of ESA, NASA, ISRO, CNSA, Roscosmos, and JAXA.